Received: 12 January 2022 | Revised: 14 March 2022 | Accepted: 6 May 2022

DOI: 10.1002/hbm.25951

RESEARCH ARTICLE

WILEY

Two distinct subtypes of obsessive compulsive disorder revealed by a framework integrating multimodal neuroimaging information

Shaoqiang Han[1,2,3,4,5,6,7,8] | Yinhuan Xu[1,2,3,4,5,6,7,8] | Hui-Rong Guo[9] | Keke Fang[10] | Yarui Wei[1,2,3,4,5,6,7,8] | Liang Liu[1,2,3,4,5,6,7,8] | Junying Cheng[1,2,3,4,5,6,7,8] | Yong Zhang[1,2,3,4,5,6,7,8] | Jingliang Cheng[1,2,3,4,5,6,7,8]

[1]Department of Magnetic Resonance Imaging, the First Affiliated Hospital of Zhengzhou University, China

[2]Key Laboratory for Functional Magnetic Resonance Imaging and Molecular Imaging of Henan Province, China

[3]Engineering Technology Research Center for Detection and Application of Brain Function of Henan Province, China

[4]Engineering Research Center of Medical Imaging Intelligent Diagnosis and Treatment of Henan Province, China

[5]Key Laboratory of Magnetic Resonance and Brain Function of Henan Province, China

[6]Key Laboratory of Brain Function and Cognitive Magnetic Resonance Imaging of Zhengzhou, China

[7]Key Laboratory of Imaging Intelligence Research Medicine of Henan Province, China

[8]Henan Engineering Research Center of Brain Function Development and Application, China

[9]Department of Psychiatry, the First Affiliated Hospital of Zhengzhou University, China

[10]Department of Pharmacy, Affiliated Cancer Hospital of Zhengzhou University, Henan Cancer Hospital, China

Correspondence
Shaoqiang Han, Department of Magnetic Resonance Imaging, the First Affiliated Hospital of Zhengzhou University, Zhengzhou, China.
Email: shaqianghan@163.com, and shaoqianghan@163.com

Funding information
Medical Science and Technology Research project of Henan province, Grant/Award Numbers: SBGJ202101013, SBGJ202102102, 201701011; Natural Science Foundation of China, Grant/Award Numbers: 62106229, 81871327, 81601467

Abstract

Patients with obsessive compulsive disorder (OCD) exhibit tremendous heterogeneity in structural and functional neuroimaging aberrance. However, most previous studies just focus on group-level aberrance of a single modality ignoring heterogeneity and multimodal features. On that account, we aimed to uncover OCD subtypes integrating structural and functional neuroimaging features with the help of a multiview learning method and examined multimodal aberrance for each subtype. Ninety-nine first-episode untreated patients with OCD and 104 matched healthy controls (HCs) undergoing structural and functional MRI were included in this study. Voxel-based morphometric and amplitude of low-frequency fluctuation (ALFF) were adopted to assess gray matter volumes (GMVs) and the spontaneous neuronal fluctuations respectively. Structural/functional distance network was obtained by calculating Euclidean distance between pairs of regional GMVs/ALFF values across patients. Similarity network fusion, one of multiview learning methods capturing shared and complementary information from multimodal data sources, was used to fuse multimodal distance networks into one fused network. Then spectral clustering was adopted to categorize patients into subtypes. As a result, two robust subtypes were

identified. These two subtypes presented opposite GMV aberrance and distinct ALFF aberrance compared with HCs while shared indistinguishable clinical and demographic features. In addition, these two subtypes exhibited opposite structure–function difference correlation reflecting distinct adaptive modifications between multimodal aberrance. Altogether, these results uncover two objective subtypes with distinct multimodal aberrance and provide a new insight into taxonomy of OCD.

KEYWORDS

heterogeneity, multimodal, multiview learning method, obsessive compulsive disorder, subtypes

1 | INTRODUCTION

Patients with obsessive compulsive disorder (OCD) demonstrate tremendous interindividual heterogeneity in terms of symptom presentations and treatment responses (Alexander et al., 1986; McKay et al., 2004). Although this heterogeneity might be resulted from factors including age of onset, comorbidity, duration of illness, there is a gradually accepted notion that mental disorders including OCD are inherently heterogeneous (P. S. W. Boedhoe et al., 2018; McKay et al., 2004). High level of heterogeneity results in conflicting findings of neuroimaging studies, hampering discovery of validated findings indicative of precision diagnosis and treatment (Bokor & Anderson, 2014). To resolve the heterogeneity, clinical psychiatrists rely exclusively on subtyping patients with OCD into categories according to clinical manifestations (McKay et al., 2004). However, taxonomy based on phenomenology cannot uncover underpinned neuroanatomical pathophysiology and presents too vague diagnostic threshold to exclude sub-threshold symptoms (Okada et al., 2015). Thus, subtypes based on symptomatology often share overlapped neuroimaging aberrance (Ravindran et al., 2020; Xia et al., 2020; Yoo et al., 2008). What is worse, the similar clinical manifestations could be caused by distinct mechanisms (Beijers et al., 2019; Goldberg, 2011). All these factors limit the impact of studies attempting to handle the heterogeneity using symptom profiles (Chand et al., 2020). To pave the way for precision medicine, it is urgent to uncover subjective subtypes directly related to biological heterogeneity using neuroimaging data (Chand et al., 2020).

The interindividual heterogeneity leads to inconsistent neuroimaging findings in mental disorders (Lv et al., 2020). The heterogeneity is acknowledged by an increasing number of researchers (Chand et al., 2020; Lv et al., 2020; Voineskos et al., 2020; Wolfers et al., 2018) and accepted as one of the leading causes resulting in conflicting findings in neuroimaging studies (Liu, Palaniyappan, et al., 2021; Wolfers et al., 2018). In OCD, although the cortico-striato-thalamo-cortical circuit is widely accepted as the core circuit, the conclusions are far from unanimous (P. S. W. Boedhoe et al., 2018; Bokor & Anderson, 2014; Saxena & Rauch, 2000). Neuroimaging studies witness reduced, increased and even no differential gray matter volumes in patients with OCD (Lázaro et al., 2011; Okasha et al., 2000). The possible reason is that group-level aberrance is not representative of most of individual patients with mental disorders (Lv et al., 2020; Sun et al., 2021; Wolfers et al., 2018). For that reason, many attempts have been made to uncover more homogeneous subtypes with distinct neuroimaging manifestations. Dwyer et al. uncover two neuroanatomical subtypes of schizophrenia improving stratification for computer-aided diagnose (Dwyer et al., 2018). Chand et al. adopting semi-supervised method reveal two robust subtypes where subtype 1 presents widespread decreased GMVs while subtype 2 presents increased GMVs in basal ganglia and internal capsule. These two subtypes challenge the widely accepted notion that schizophrenia is characterized by general brain volume loss (Chand et al., 2020), help to deepen our understanding of mechanism and move toward targeted treatment (Varol et al., 2017). Nonetheless, these studies only focus on a single neuroimaging modality alone (Chand et al., 2020; Drysdale et al., 2017; Sundermann et al., 2014).

Mental disorders are accompanied by structural and functional aberrance reflecting different sides of pathological features. In OCD, beyond structural aberrance, patients with OCD demonstrate functional abnormalities in regional activity and interregional functional coordination (Soriano-Mas, 2021; Stein et al., 2019; Veltman, 2021). In addition, brain structure and function differences are not independent of each other and neither of them can delineate the complete picture of the pathomechanism of mental disorders. For example, cognitive impairment is related to multimodal signatures in schizophrenia (Sui et al., 2018). The coupling between functional and structural connectivity in numbers of brain networks is altered in schizophrenia (Skudlarski et al., 2010). Machine learning frameworks combing multi neuroimaging modalities exhibit better diagnostic performance than that using a single modality (Du et al., 2012; Lei & Pinaya, 2020; Ota et al., 2013). Combing multimodal information provides an integrated insight into the pathophysiology of mental disorders. Nonetheless, it is a challenge integrating multimodal data sources (Mišić & Sporns, 2016). Recent progress in techniques such as multi-view learning methods makes it possible that exploiting the complementary information from different data sources (S. Fan et al., 2020; Rai et al., 2017). As one of these methods, similarity network fusion (SNF) (Wang et al., 2014) is proved to yield a balanced representation of multiview data sources (Markello et al., 2021). Using SNF, Ross et al. integrate multimodal data sources and successfully uncover putative subtypes of Parkinson's disease, suggesting the potential of SNF for

integrating multimodal data in heterogeneous disorders (Markello et al., 2021).

In this study, we aimed to uncover potential subtypes by integrating structural and functional MRI data with the help of SNF and examine multimodal aberrance in each subtype of OCD. Structural T1-weight MRI and resting-state functional MRI data were collected from first-episode and untreated patients with OCD ($n = 99$) and matched healthy controls ($n = 104$). Voxel-based morphometric and amplitude of low-frequency fluctuation (ALFF) were adopted to assess regional gray matter volumes (GMVs) and the spontaneous neuronal fluctuations, respectively (Ashburner & Friston, 2000; Yu-Feng et al., 2007). We would show that our proposed framework could identify putative subtypes of OCD by integrating multimodal information (GMV and ALFF). Then, we examined multimodal and clinical phenotypes for each subtype.

2 | MATERIALS AND METHODS

2.1 | Sample

Written informed consents were obtained from all participants before experiment. The study was approved by the research ethical committee of the First Affiliated Hospital of Zhengzhou University. We recruited patients with OCD ($n = 99$) and matched healthy controls (HCs, $n = 104$). Patients were recruited from out-patient services of Department of Psychiatry, the First Affiliated Hospital of Zhengzhou University. The diagnosis was done by two experienced psychiatrists according to Diagnostic and Statistical Manual of Mental Disorders, Fifth Edition (DSM-V) for OCD. All patients were drag-naive and first-episode. One patient would be excluded if it was comorbidity with other mental/psychotic disorders, suffering from nervous system disease/brain trauma, or its first degree relatives having a history with mental illness/neurological disease. Yale–Brown Obsessive Compulsive Scale (Y-BOCS) was used to evaluate severity of symptoms (Goodman et al., 1989). All participants were Han Chinese and right-handed and must meet the additional exclusion criteria: (1) Taking drugs such as anesthesia, sleeping or analgesia in the past 1 month; (2) substance abuse; (3) a history of brain tumor, trauma, surgery or other organic body disease; (4) suffering from cardiovascular diseases, diabetes or hypertension; (5) contraindications for MRI scanning; and (6) other structural brain abnormalities. The data acquisition, preprocessing steps (Han et al., 2018; Han et al., 2020), voxel-based morphometry (Ashburner, 2009; Han, Chen, et al., 2021; Han, Zheng, et al., 2021), ALFF, and quality assurance were included in supplementary information S1.

2.2 | Subtyping patients with OCD

We aimed to uncover potential subtypes of OCD integrating structural and functional neuroimaging modality. Main steps included: (1). Constructing structural and functional distance network by calculating Euclidean distance between pairs of $M \times 1$ (M, the number of brain regions defined in brain atlas) regional GMVs/ALFF values across patients. Thus, two $N \times N$ (N, the number of patients) distance networks were obtained from GMV and ALFF respectively; (2) fusing multimodal information using similarity network fusion (SNF). SNF integrated multimodal distance networks into one fused network that captured shared and complementary information from multimodal datasets (Wang et al., 2014). There were two free parameters to be considered in SNF: K and μ. K controlled the neighbors of one node (subject) to be considered when constructing fused networks where a larger K would result in a more sparsely connected network or vice versa. μ determined the weights of edges between nodes (subjects) in the fused network. A smaller μ would only keep the strongest edges while a larger one would endure the weaker edges in the fused network (Wang et al., 2014). The recommended ranges of K and μ were [10, 30] and [0.3, 0.8], respectively (Wang et al., 2014). The optimal combination of K and μ was determined according to following procedures (see below); (3) once we obtained the fused network based on the optimal combination of K and μ, spectral clustering was adopted to divided patients into subtypes based on the fused network. The number of clusters was determined through eigen-gap (Wang et al., 2014). These subtyping procedures were done with 268 regions brain atlas and validated with 200 regions brain atlas (Craddock et al., 2012; Shen et al., 2013). Adjusted rand index (ARI) was used to measure the consistency of subtyping results based on these two brain atlases. The workflow was included in Figure 1.

Inspired by one previous study (Markello et al., 2021), we proposed an strategy to determine the optimal combination of K and μ avoiding an arbitrary decision. We assumed that the optimal combinations should generate stable subtyping results. That is to say, small perturbations in one of parameters (K or μ) did not dramatically change the subtyping results. We searched optimal combined of K and μ from recommended range (K: 10–30, interval = 1; μ: 0.3–0.8, interval = 0.1). For each combination, we obtained subtyping results following the step (3) (mentioned before). Here, we defined a similarity matrix to measure the consistency of subtyping results for each node in the hyperparameter space. Specially, for a given node "a" (one combination of K and μ) in the hyperparameter space, we identified its four neighbors (e.g., "a" and its four neighbors in Figure 1b). ARI was used to measure the similarity between subtyping results obtained from each pairs of five nodes (in all, $C(5,2) = 10$ pairs). The local similarity of "a" was defined as the average ARI value of subtyping results obtained from these 10 combinations. If the number of neighbors was less than 4 (for the node at the edge of the hyperparameter space), we used the actual number of neighbors. A larger local similarity value meant a more stable subtyping result. The largest values in the similarity matrix were found out. After that, we calculated consistency values between each pairs of structural, functional and the fused distance network for each node with the largest local similarity values. Among these, we picked the optimal combination where the average consistency value was the largest. The consistency between each pair of distance networks was measured with normalized mutual information (NMI) (Strehl, & Ghosh, 2003).

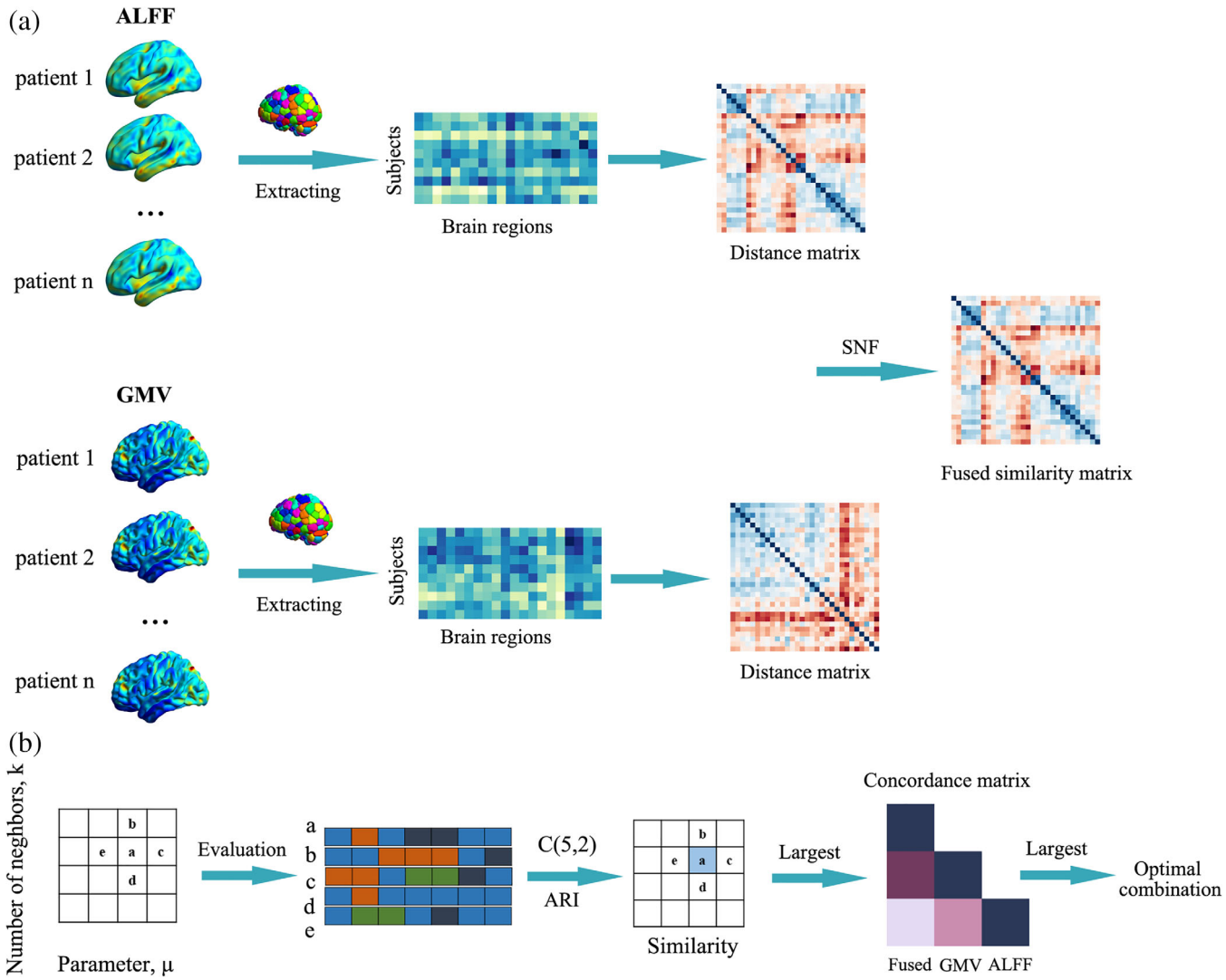

FIGURE 1 The workflow of subtyping strategy integrating multimodal information. (a) Multimodal (amplitude of low-frequency fluctuation [ALFF] and gray matter volume [GMV]) distance networks were constructed and then integrated into one fused network using similarity network fusion (SNF). (b) Strategy to determine the optimal combination of K and μ. Here, we defined a similarity matrix to measure the consistency of subtyping results for each node in the hyperparameter space. For a given node "a" in hyperparameter space and its four neighbors (b, c, d, and e), we obtained their corresponding subtyping results. Adjusted rand index (ARI) was used to measure the similarity between subtyping results obtained from each pairs of five nodes (C(5,2) = 10). The local similarity of "a" was defined as the average ARI value of each pairs of subtyping results. A larger local similarity value meant a more stable subtyping result. The largest values in the similarity matrix were found out. Then we calculated consistency values between each pairs of structural, functional and the fused distance network for each node with the largest local similarity values (yielding a concordance matrix for each node). Among these, we picked the node where the average consistency value was the largest.

2.3 | Clinical and multimodal examination of OCD subtypes

First, we examined clinical and demographic features for each subtype. Age, sex, education level, duration of illness, and TIV were compared between each pairs of OCD subtypes using two sample *t* test. Then, we examined the voxel-wise multimodal aberrance for each subtype compared with HCs using two sample *t* test in SPM12 (https://www.fil.ion.ucl.ac.uk/spm/software/spm12/). In this procedure, age, sex, educational level, and TIV were treated as covariates. Reported results were corrected with FDR ($p < .05$). As a validation, we also calculated the voxel-wise multimodal aberrance based on subtyping results of 200 region brain atlas in construction of distance networks. The spatial correlations between multimodal aberrance (unthresholded voxel-wise t-statistic maps) of 268 regions brain atlas and that of 200 regions brain atlas were calculated to evaluate the consistency of multimodal voxel-wise aberrance.

In addition, to further inquire the reliability of voxel-wise results, we randomly selected 80% of patients and HCs, respectively, and performed voxel-wise statistical analysis for each subtype (Liu

TABLE 1 Sample demographics

	HC ($N = 104$)	OCD ($N = 99$)	p
Male, No. (%)	51 (49.04)	52 (52.53)	.99[a]
Age, mean (SD) [range], years	23.14 (5.64) [16–43]	23.16 (9.34) [12–49]	.99[b]
Educational level, mean (SD), years	15.21 (3.17)	11.95 (3.04)	<.01[b]
Duration of illness, mean (SD), m	-	48.08 (57.61)	
Y-BOCS score, mean (SD)	-	21.73 (6.91)	
TIV, mean (SD),10^3	1.54 (0.13)	1.55 (0.15)	.68[b]
IQR, mean (SD)	2.08 (0.13)	2.08 (0.15)	.71[b]
SNR, mean (SD)	207.48 (39.75)	216.31 (44.56)	.14[b]
Mean FD, mean (SD)	0.11 (0.05)	0.12 (0.10)	.39[b]

Abbreviations: HC, healthy control; IQR, imaging quality rating; mean FD, mean frame-wise displacement; OCD, obsessive–compulsive disorder; SNR0, signal-to-noise ratios; TIV, total intracranial volume; Y-BOCS: Yale–Brown Obsessive Compulsive Scale.
[a]Chi-square t-test.
[b]Two-tailed two sample t-test.

et al., 2020). Then, the spatial correlation between the new GMV/ALFF aberrance (unthresholded voxel-wise t-statistic map) and that we reported was obtained. This procedure was done in subtyping results based on 268 regions brain atlas and repeated 100 times.

2.4 | Validation analysis

To investigate the reliability of our results, we adopted various strategies. (1) Using different brain atlases when a brain atlas was needed. Consistency of results obtained with different brain atlases was inquired with proper methods such as spatial correlation and ARI; (2) randomly selecting sub-dataset to validate the voxel-wise aberrance results. The details were included in corresponding parts in method section.

2.5 | Association between multimodal aberrance

To explore whether there was association between structural and functional aberrance in identified subtypes. We calculated regional GMV/ALFF aberrance (unthresholded t-statistic maps) based on brain atlas (268 and 200 brain atlases) thus yielding two t-value vectors. Then, the Pearson correlation between them was obtained to measure the association between GMV and ALFF aberrance. This procedure was done in each subtype and all patients.

3 | RESULTS

3.1 | Clinical demographics

The demographics information was included in Table 1. These was no significant difference between patients with OCD and HCs in terms of age, TIV, IQR and sex (all p values > .05). Patients with OCD had less years of education than HCs.

3.2 | Two robust subtypes are identified by fused network

After searching the hyperparameter space, a series of combinations of K and μ were identified where the local similarity reached 1 suggesting fairly stable performance against to small perturbations (the similarity matrix was drawn in Figure S1). Among these, we further selected combination having the highest consistency value between each pairs of structural, functional and fused distance networks. Using this optimal combination of K and μ, two subtypes of OCD were identified by spectral clustering based on the fused network (OCD 1 and OCD 2). When 200 regions brain atlas was used, the optimal number of subtypes was also 2. The ARI between subtyping results based on different brain atlases was 0.960 declaring a good consistency.

3.3 | Two OCD subtypes demonstrate distinct multimodal aberrance

These was no significant difference between these two OCD subtypes in terms of age, sex, educational level, TIV and the total score of Y-BOCS (all p values > .05). However, these two OCD subtypes demonstrated remarkably distinct GMV/ALFF aberrance compared with HCs. Specially, OCD 1 showed decreased GMV while OCD 2 presented increased GMV throughout the brain ($p < .05$, FDR corrected). However, when mixed up, all patients demonstrated no differential GMV compared with HCs. On the other hand, OCD 1 showed decreased ALFF in cerebellum while increased ALFF in right inferior parietal lobe. OCD 2 exhibited altered ALFF in numbers of brain regions including thalamus, hippocampus, cerebellum, occipital gyrus and frontal gyrus (Figure 2, Table S1). We also obtained ALFF aberrance in all patients with OCD compared with HCs. When mixed together, all patients demonstrated increased ALFF in inferior parietal lobule and decreased ALFF in brain regions such as motor regions, cerebellum, and precuneus (Figure S2 and Table S2). The multimodal difference was drawn in Figure S3.

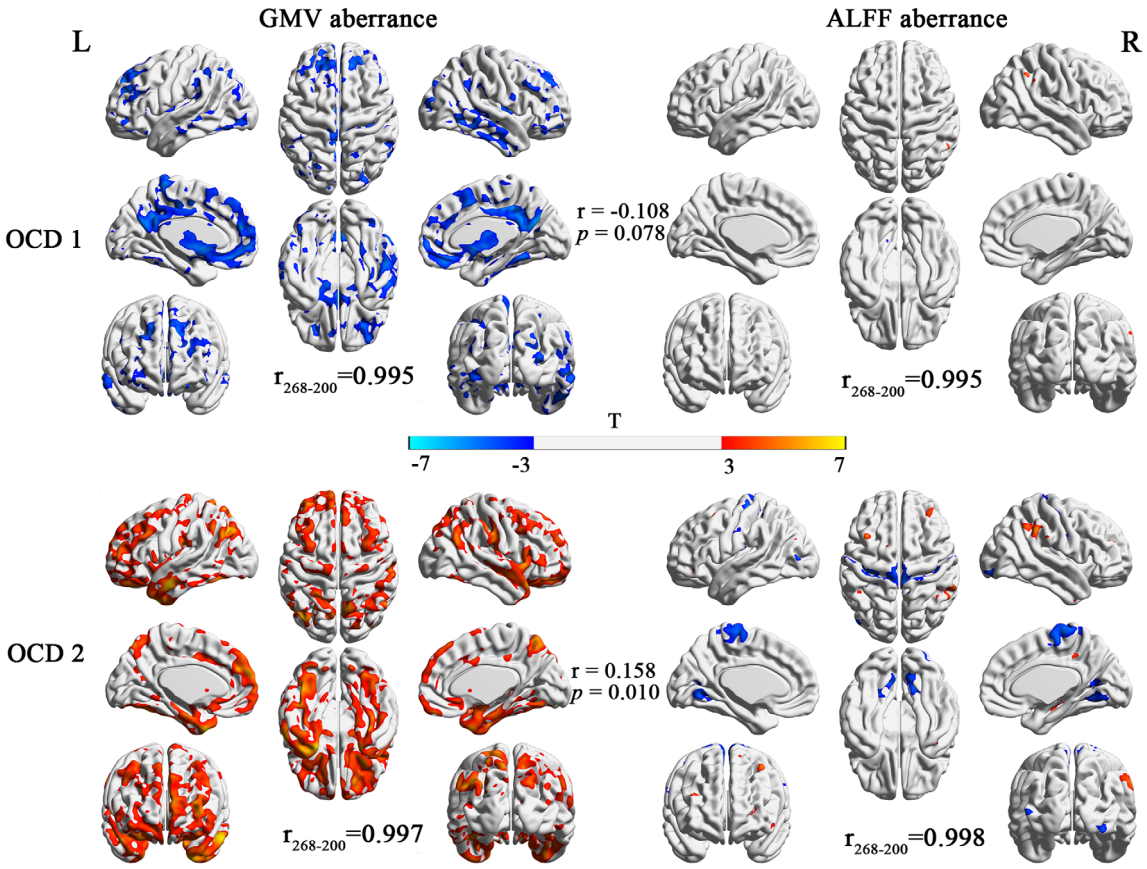

FIGURE 2 Gray matter volume (GMV) and amplitude of low-frequency fluctuation (ALFF) aberrance in each subtype of obsessive compulsive disorder (OCD). The $r_{268\text{-}200}$ represented the spatial correlation between multimodal aberrance based on different brain atlases. The *r* represented the spatial correlation between structural and functional aberrance for each subtype of OCD.

3.4 | Validation results

The spatial correlations between multimodal voxel-wise aberrance of 268 and 200 regions brain atlas in each subtype were summarized in Table S3 and Figure 2 ($r_{268\text{-}200}$). The high correlation coefficients suggested a good agreement between voxel-wise aberrance obtained from different brain atlases. To exclude the chance that the voxel-wise aberrance was induced by few subjects, we randomly selected a certain percentage of patients and HCs and obtained voxel-wise aberrance in this sub-dataset. The spatial correlation was calculated to measure the consistency between voxel-wise aberrance results. Our results suggested a good reproducibility of multimodal aberrance in each subtype. The distribution of spatial correlations was drawn in Figure 3 and summarized in Table S4.

3.5 | Spatial correlation between structural and functional aberrance

We also investigated the association between structural and functional aberrance in each subtype of OCD. In OCD 1, there was a negative correlation between ALFF and VBM aberrance ($r = -.011$, $p = .078$ for 268 regions brain atlas; $r = -.193$, $p = .006$ for 200 regions brain atlas). In contrast, ALFF aberrance presented significant positive correlation with GMV aberrance ($r = 0.156$, $p = .010$ for 268 regions brain atlas; $r = .243$, $p < .001$ for 200 regions brain atlas) in OCD 2. Once all patients were mixed, we did not observe significant correlation between GMV and ALFF aberrance (Figure 4, Table S3).

4 | DISCUSSION

To uncover subtypes of OCD, we proposed a subtyping framework integrating structural and functional information. Using this framework, two robust subtypes of OCD were identified. These two subtypes demonstrated remarkably distinct multimodal differences while shared indistinguishable clinical and demographic features. Compared with HCs, OCD 1 exhibited decreased GMVs in widely distributed brain regions. On the contrary, OCD 2 exhibited increased GMVs throughout the brain. When comparing all patients with HCs, we did not observe significant differential GMV. With regard to ALFF, OCD 1 presented decreased ALFF in cerebellum anterior lobe and increased ALFF in inferior parietal lobule. OCD 2 demonstrated increased ALFF in brain regions including hippocampus, thalamus, inferior temporal lobe and middle frontal gyrus while decreased ALFF

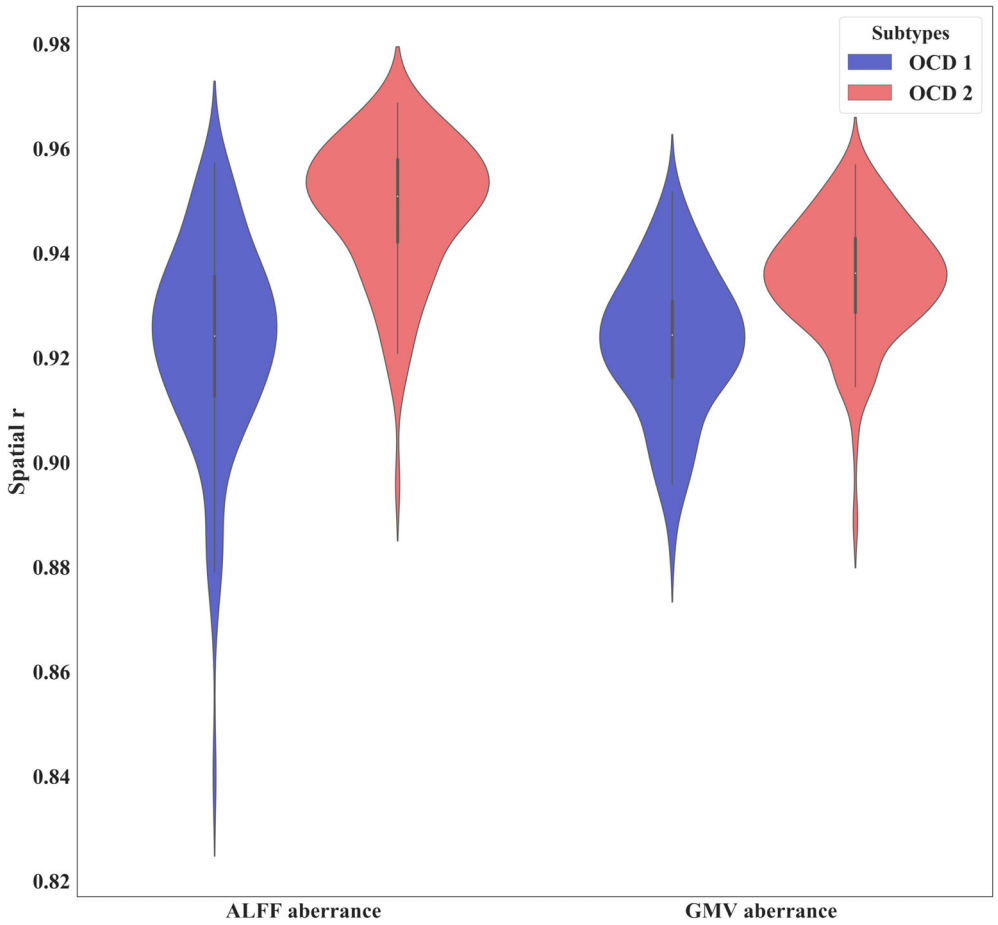

FIGURE 3 Spatial correlation between gray matter volume (GMV)/amplitude of low-frequency fluctuation (ALFF) aberrance obtained from randomly selected sub-dataset with that from the whole dataset.

in motor area, cerebellum, and calcarine. In addition, these two subtypes exhibited opposite structure–function difference association.

Our framework integrating structural and functional data revealed two reproducible subtypes of OCD. Almost all previous studies using neuroimaging data subtyped patients with mental disorders based on one MRI modality (Chand et al., 2020; Drysdale et al., 2017; Sundermann et al., 2014; Varol et al., 2017). These studies ignored the multimodal nature in mental disorders like OCD (Soriano-Mas, 2021; Veltman, 2021). To our knowledge, it was the first attempt using multimodal MRI data to uncover putative subtypes of OCD. Although we only combined structural and functional data in this study, this framework could integrate more modal data sources, such as transporter binding and protein assays (Markello et al., 2021). Avoiding an arbitrary setting, our framework determined the number of subtypes automatically. We further investigated the consistency of subtyping results between different brain atlases. Validation results showed that the subtyping results could be reproducible across different brain atlases and in randomly selected subgroup. These results suggested the feasibility of our framework in subtyping patients with mental disorders like OCD.

Even factors like medicine statue and comorbidity were well controlled, patients with OCD exhibited tremendous heterogeneity reflected in multimodal aberrance. These identified two subtypes of OCD demonstrated distinct structural and functional aberrance. Especially, these two subtypes exhibited completely opposite structural differences compared with HCs in distributed brain regions while shared indistinguishable clinical symptoms and demographic features. Nonetheless, when mixed together, all patients presented no difference with HCs. We did not observe any difference in terms of age and illness duration between these two subtypes. Please note that this result did not necessary deny the effect of these factors. Actually, studies found that age and illness duration drove enlargement of striatal areas (P. S. Boedhoe et al., 2017; de Wit et al., 2014). One plausible explanation was that the effect of age/illness duration could be ignored when compared with that of inherent heterogeneity between these subtypes revealed in this study. Nowadays, clinical therapeutic schedule was often determined according to symptom profile. Specific symptoms were likely to response distinctly to treatment (Komulainen et al., 2021; Starcevic & Brakoulias, 2008). For example, 75% of patients cleaning/checking received cognitive behavior therapy (Ball et al., 1996) while hoarding symptoms were consistently found to respond less well to cognitive behavioral therapy and to pharmacotherapy (McKay et al., 2004). Among symptoms of OCD, checking and cleaning responded better to treatment than others (McKay et al., 2004). One possible reason was that works had been done to increase rates of improvement of specific symptoms while the others that relatively understudied would be less responsive to current treatments (McKay et al., 2004). According to symptom profiles, these two

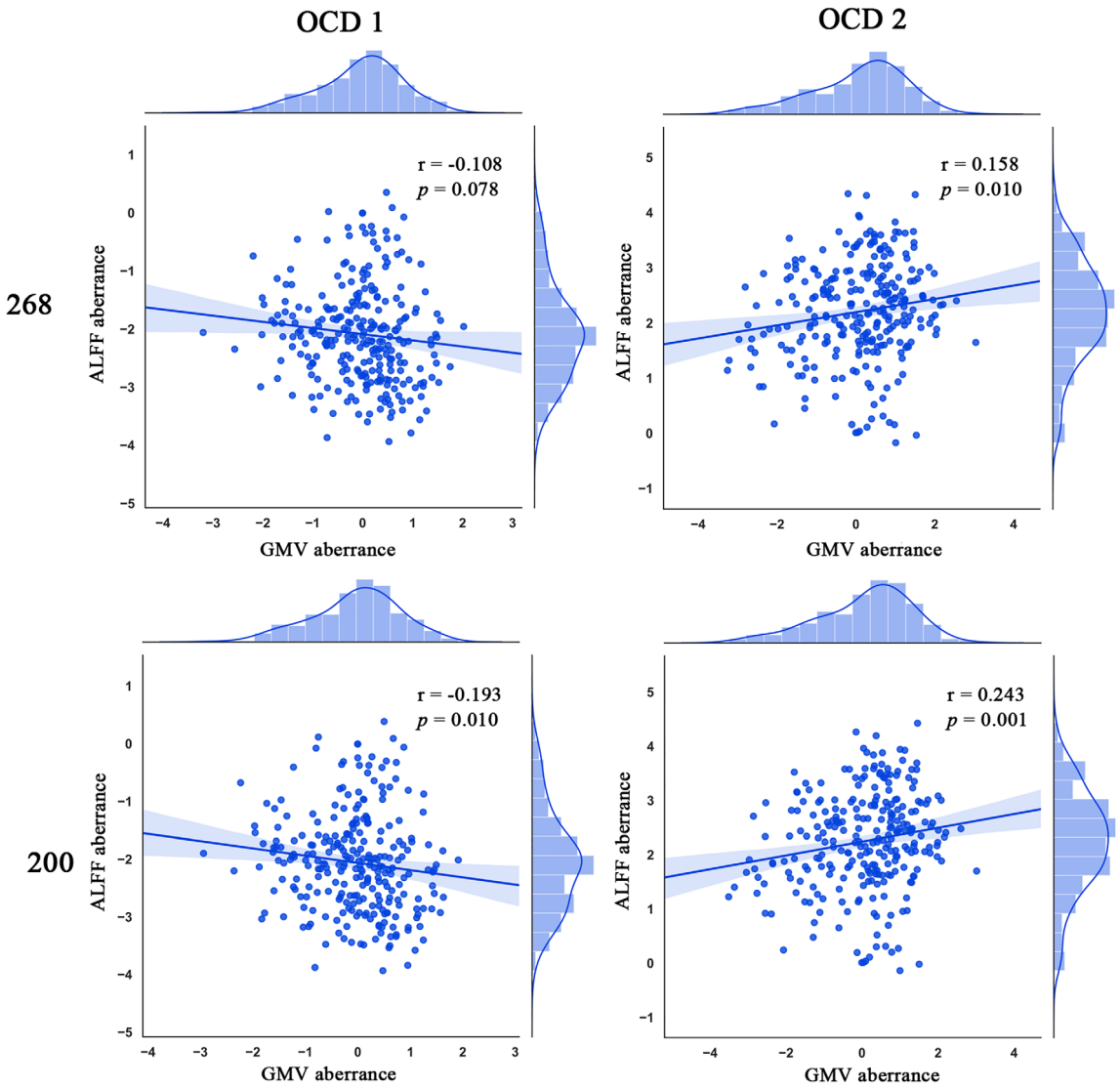

FIGURE 4 Spatial correlation between gray matter volume (GMV) and amplitude of low-frequency fluctuation (ALFF) aberrance. Spatial correlation was based on 268/200 brain atlas separately.

subtypes might be likely to treated with the same therapeutic regimen in clinical. However, exhibiting remarkable multimodal aberrance, these two subtypes were expected to respond distinctly to treatment. This assumption could be verified in the future. In general, our framework revealed subtypes not otherwise detectible by symptom representations and provided a new insight into taxonomy of OCD independent of symptom representations.

Consistent with the notion that the etiology of OCD might involve more widely distributed largescale brain systems, such as limbic system and the salience network, these two subtypes exhibited abnormal GMVs in distributed brain regions (Alexander et al., 1986; P. S. W. Boedhoe et al., 2018; Glahn et al., 2015; Menzies et al., 2008). Nonetheless, they exhibited completely opposite structural aberrance pattern, might explaining inconsistent findings in previous studies such as orbitofrontal gyrus and right anterior insula (P. S. Boedhoe et al., 2017; P. S. W. Boedhoe et al., 2018; Lázaro et al., 2011; Okasha et al., 2000; Rotge et al., 2009). Studies with functional imaging studies revealed hypermetabolism and increased cerebral bold flow in orbitofrontal gyrus (Saxena et al., 1998; Saxena & Rauch, 2000; Swedo et al., 1992). In accordance with these findings, volume of orbitofrontal gyrus was found increased in OCD (Kim et al., 2001; Pujol et al., 2004; Szeszko et al., 2008). However, decreased volume of this brain region was also reported (Pujol et al., 2004; van den Heuvel et al., 2009). As another key region in OCD, right anterior insula was suggested to be respond for the poorer inhibitory control in OCD (J. Fan et al., 2016). GMVs were found both increased (Nishida et al., 2011; Yoo et al., 2008) and decreased in right anterior insula (Besiroglu et al., 2011; Subirà et al., 2013). In addition to opposite structural difference, these two subtypes also exhibited distinct altered spontaneous brain activity in brain regions distributed in networks/circuits frequently reported including orbitofronto-striatal circuit (Menzies et al., 2008), frontoparietal network (Eng

et al., 2015) and cerebellum (Hou et al., 2012; Liu, Bu, et al., 2021). These conflicting findings were often attributed to medicine exposure, methodological differences, comorbidity or illness duration (P. S. Boedhoe et al., 2017; P. S. W. Boedhoe et al., 2018; Veltman, 2021). However, our results suggested the heterogeneity might be inherent to OCD. Recently, researchers began to acknowledge the high heterogeneity and realize that group-level difference of brain structure was not representative of every patient in mental disorders (Liu, Palaniyappan, et al., 2021; Lv et al., 2020; Wolfers et al., 2018; Wolfers et al., 2020). However, to our knowledge, only limited studies focused on structural aberrance in subtypes of OCD (e.g., children vs. adult, contamination vs. aggressive) (P. S. Boedhoe et al., 2017; P. S. W. Boedhoe et al., 2018; Yoo et al., 2008). Future researchers might be pay more attention on more homogeneous samples even individualized aberrance in the study of OCD.

Another notable finding was the opposite association between structural and functional aberrance in each subtype of OCD. Brain structure and function reflecting different perspectives of brain function were not independent. Even the detail association between brain structure and function remained unknown, it was suggested that anatomical architecture constrained brain function and that brain function interactions could be predicted from brain structure (Honey et al., 2009). On the contrary, function of brain such as functional coordination was found to also expert influence on structural connections through the plasticity mechanism (Hagmann et al., 2008; Honey et al., 2009). The coupling of brain structure and function was found to be altered in brain disorders and development. For example, schizophrenia demonstrated a decoupling interaction between structural and functional connectivity in the DMN and task-positive network (Skudlarski et al., 2010). Similar findings were found in bipolar disorder (Jiang et al., 2020) and attention-deficit hyperactivity disorder (Hearne & Lin, 2021). Structure–function coupling was remodeled to support functional specialization and cognition during adolescent brain development (Baum et al., 2020). The opposite structure–function correlations might reflect distinct adaptive modifications between structural and functional aberrance in subtypes of OCD. We hypothesized that these two subtypes would present distinct altered structure–function coupling. Future studies could confirm this hypothesis.

4.1 | Limitations and future directions

Numbers of limitations in this study were worth mentioning. First, even we used multiple strategies to confirm the reliability of these results. These results were obtained in a single dataset, one more dataset was needed to validate these results. Second, factors such as body mass index, alcohol/cigarette use were not controlled in this study, future studies could evaluate their effects on these results. Third, we did not include patients with late onset OCD; thus, we could not know whether our conclusion held true for late onset OCD. Fourth, we did not record enough clinical information (such as neuropsychological performance and pharmacological treatment), thus we could not investigate the relationship between the identified subtypes and obsessive dimensions.

5 | CONCLUSION

With the help of a multiview learning method named SNF, we proposed a novel framework integrating structural and functional information and successfully uncovered two subject subtypes of OCD. These two subtypes presented totally opposite GMV difference and distinct ALFF aberrance compared with HCs while shared indistinguishable clinical and demographic features. These results suggested that these two subtypes were otherwise obscured by taxonomy based on phenomenology. In addition, these two subtypes demonstrated opposite spatial correlations between structural and functional aberrance. Altogether, our results revealed two distinct multimodal OCD subtypes facilitating a new insight into clinical precision diagnostics.

ACKNOWLEDGMENTS

This research study was supported by the Natural Science Foundation of China (81601467, 81871327, 62106229) and Medical Science and Technology Research project of Henan province (201701011, SBGJ202102102, SBGJ202101013).

CONFLICT OF INTEREST

All authors declared no conflict of interest.

DATA AVAILABILITY STATEMENT

Data sharing is not applicable to this article as no new data were created or analyzed.

ORCID

Shaoqiang Han https://orcid.org/0000-0001-7331-0315
Yarui Wei https://orcid.org/0000-0002-4264-6374
Yong Zhang https://orcid.org/0000-0003-4892-6614
Jingliang Cheng https://orcid.org/0000-0002-6996-329X

REFERENCES

Alexander, G. E., DeLong, M. R., & Strick, P. L. (1986). Parallel organization of functionally segregated circuits linking basal ganglia and cortex. *Annual Review of Neuroscience*, *9*, 357–381. https://doi.org/10.1146/annurev.ne.09.030186.002041

Ashburner, J. (2009). Computational anatomy with the SPM software. *Magnetic Resonance Imaging*, *27*(8), 1163–1174. https://doi.org/10.1016/j.mri.2009.01.006

Ashburner, J., & Friston, K. J. (2000). Voxel-based morphometry--the methods. *NeuroImage*, *11*(6 Pt 1), 805–821. https://doi.org/10.1006/nimg.2000.0582

Ball, S. G., Baer, L., & Otto, M. W. (1996). Symptom subtypes of obsessive-compulsive disorder in behavioral treatment studies: A quantitative review. *Behaviour Research and Therapy*, *34*(1), 47–51. https://doi.org/10.1016/0005-7967(95)00047-2

Baum, G. L., Cui, Z., Roalf, D. R., Ciric, R., Betzel, R. F., Larsen, B., Cieslak, M., Cook, P. A., Xia, C. H., Moore, T. M., Ruparel, K., Oathes, D. J., Alexander-Bloch, A. F., Shinohara, R. T., Raznahan, A., Gur, R. E., Gur, R. C., Bassett, D. S., & Satterthwaite, T. D. (2020).

Development of structure-function coupling in human brain networks during youth. *Biological Sciences*, *117*(1), 771–778. https://doi.org/10.1073/pnas.1912034117

Beijers, L., Wardenaar, K. J., van Loo, H. M., & Schoevers, R. A. (2019). Data-driven biological subtypes of depression: Systematic review of biological approaches to depression subtyping. *Molecular Psychiatry*, *24*(6), 888–900. https://doi.org/10.1038/s41380-019-0385-5

Besiroglu, L., Sozen, M., Ozbebit, O., Avcu, S., Selvi, Y., Bora, A., Atli, A., Unal, O., & Bulut, M. D. (2011). The involvement of distinct neural systems in patients with obsessive-compulsive disorder with autogenous and reactive obsessions. *Acta Psychiatrica Scandinavica*, *124*(2), 141–151. https://doi.org/10.1111/j.1600-0447.2011.01726.x

Boedhoe, P. S., Schmaal, L., Abe, Y., Ameis, S. H., Arnold, P. D., Batistuzzo, M. C., Benedetti, F., Beucke, J. C., Bollettini, I., Bose, A., Brem, S., Calvo, A., Cheng, Y., Cho, K. I. K., Dallaspezia, S., Denys, D., Fitzgerald, K. D., Fouche, J. P., Giménez, M., … Zhao, Q. (2017). Distinct subcortical volume alterations in pediatric and adult OCD: A worldwide meta- and mega-analysis. *The American Journal of Psychiatry*, *174*(1), 60–69. https://doi.org/10.1176/appi.ajp.2016.16020201

Boedhoe, P. S. W., Schmaal, L., Abe, Y., Alonso, P., Ameis, S. H., Anticevic, A., Arnold, P. D., Batistuzzo, M. C., Benedetti, F., Beucke, J. C., Bollettini, I., Bose, A., Brem, S., Calvo, A., Calvo, R., Cheng, Y., Cho, K. I. K., Ciullo, V., Dallaspezia, S., … van den Heuvel, O. A. (2018). Cortical abnormalities associated with pediatric and adult obsessive-compulsive disorder: Findings from the ENIGMA Obsessive-Compulsive Disorder Working Group. *The American Journal of Psychiatry*, *175*(5), 453–462. https://doi.org/10.1176/appi.ajp.2017.17050485

Bokor, G., & Anderson, P. D. (2014). Obsessive-compulsive disorder. *Journal of Pharmacy Practice*, *27*(2), 116–130. https://doi.org/10.1177/0897190014521996

Chand, G. B., Dwyer, D. B., Erus, G., Sotiras, A., Varol, E., Srinivasan, D., Doshi, J., Pomponio, R., Pigoni, A., Dazzan, P., Kahn, R. S., Schnack, H. G., Zanetti, M. V., Meisenzahl, E., Busatto, G. F., Crespo-Facorro, B., Pantelis, C., Wood, S. J., Zhuo, C., … Davatzikos, C. (2020). Two distinct neuroanatomical subtypes of schizophrenia revealed using machine learning. *Brain*, *143*(3), 1027–1038. https://doi.org/10.1093/brain/awaa025

Craddock, R. C., James, G. A., Holtzheimer, P. E., Hu, X. P., & Mayberg, H. S. (2012). A whole brain fMRI atlas generated via spatially constrained spectral clustering. *Human Brain Mapping*, *33*(8), 1914–1928. https://doi.org/10.1002/hbm.21333

de Wit, S. J., Alonso, P., Schweren, L., Mataix-Cols, D., Lochner, C., Menchón, J. M., Stein, D. J., Fouche, J. P., Soriano-Mas, C., Sato, J. R., Hoexter, M. Q., Denys, D., Nakamae, T., Nishida, S., Kwon, J. S., Jang, J. H., Busatto, G. F., Cardoner, N., Cath, D. C., … van den Heuvel, O. A. (2014). Multicenter voxel-based morphometry mega-analysis of structural brain scans in obsessive-compulsive disorder. *The American Journal of Psychiatry*, *171*(3), 340–349. https://doi.org/10.1176/appi.ajp.2013.13040574

Drysdale, A. T., Grosenick, L., Downar, J., Dunlop, K., Mansouri, F., Meng, Y., Fetcho, R. N., Zebley, B., Oathes, D. J., Etkin, A., Schatzberg, A. F., Sudheimer, K., Keller, J., Mayberg, H. S., Gunning, F. M., Alexopoulos, G. S., Fox, M. D., Pascual-Leone, A., Voss, H. U., … Liston, C. (2017). Resting-state connectivity biomarkers define neurophysiological subtypes of depression. *Nature Medicine*, *23*(1), 28–38. https://doi.org/10.1038/nm.4246

du, W., Calhoun, V. D., Li, H., Ma, S., Eichele, T., Kiehl, K. A., Pearlson, G. D., & Adali, T. (2012). High classification accuracy for schizophrenia with rest and task FMRI data. *Frontiers in Human Neuroscience*, *6*, 145. https://doi.org/10.3389/fnhum.2012.00145

Dwyer, D. B., Cabral, C., Kambeitz-Ilankovic, L., Sanfelici, R., Kambeitz, J., Calhoun, V., Falkai, P., Pantelis, C., Meisenzahl, E., & Koutsouleris, N. (2018). Brain subtyping enhances the neuroanatomical discrimination of schizophrenia. *Schizophrenia Bulletin*, *44*(5), 1060–1069. https://doi.org/10.1093/schbul/sby008

Eng, G. K., Sim, K., & Chen, S. H. (2015). Meta-analytic investigations of structural grey matter, executive domain-related functional activations, and white matter diffusivity in obsessive compulsive disorder: An integrative review. *Neuroscience and Biobehavioral Reviews*, *52*, 233–257. https://doi.org/10.1016/j.neubiorev.2015.03.002

Fan, J., Liu, W., Lei, H., Cai, L., Zhong, M., Dong, J., Zhou, C., & Zhu, X. (2016). Components of inhibition in autogenous- and reactive-type obsessive-compulsive disorder: Dissociation of interference control. *Biological Psychology*, *117*, 117–130. https://doi.org/10.1016/j.biopsycho.2016.03.008

Fan, S., Wang, X., Shi, C., Lu, E., Lin, K., & Wang, B. (2020). One2Multi graph autoencoder for multi-view graph clustering. In *Paper presented at the proceedings of the web conference 2020*. https://doi.org/10.1145/3366423.3380079

Glahn, A., Prell, T., Grosskreutz, J., Peschel, T., & Müller-Vahl, K. R. (2015). Obsessive-compulsive disorder is a heterogeneous disorder: Evidence from diffusion tensor imaging and magnetization transfer imaging. *BMC Psychiatry*, *15*, 135. https://doi.org/10.1186/s12888-015-0535-5

Goldberg, D. (2011). The heterogeneity of "major depression". *World Psychiatry*, *10*(3), 226–228. https://doi.org/10.1002/j.2051-5545.2011.tb00061.x

Goodman, W. K., Price, L. H., Rasmussen, S. A., Mazure, C., Fleischmann, R. L., Hill, C. L., Heninger, G. R., & Charney, D. S. (1989). The Yale-Brown Obsessive Compulsive Scale. I. Development, use, and reliability. *Archives of General Psychiatry*, *46*(11), 1006–1011. https://doi.org/10.1001/archpsyc.1989.01810110048007

Hagmann, P., Cammoun, L., Gigandet, X., Meuli, R., Honey, C. J., Wedeen, V. J., & Sporns, O. (2008). Mapping the structural core of human cerebral cortex. *PLoS Biology*, *6*(7), e159. https://doi.org/10.1371/journal.pbio.0060159

Han, S., Chen, Y., Zheng, R., Li, S., Jiang, Y., Wang, C., Fang, K., Yang, Z., Liu, L., Zhou, B., Wei, Y., Pang, J., Li, H., Zhang, Y., & Cheng, J. (2021). The stage-specifically accelerated brain aging in never-treated first-episode patients with depression. *Human Brain Mapping*, *42*(11), 3656–3666. https://doi.org/10.1002/hbm.25460

Han, S., Cui, Q., Wang, X., Li, L., Li, D., He, Z., Guo, X., Fan, Y. S., Guo, J., Sheng, W., Lu, F., & Chen, H. (2020). Resting state functional network switching rate is differently altered in bipolar disorder and major depressive disorder. *Human Brain Mapping*, *41*(12), 3295–3304. https://doi.org/10.1002/hbm.25017

Han, S., He, Z., Duan, X., Tang, Q., Chen, Y., Yang, Y., Pang, Y., Nan, X., Cui, Q., & Chen, H. (2018). Dysfunctional connectivity between raphe nucleus and subcortical regions presented opposite differences in bipolar disorder and major depressive disorder. *Progress in Neuro-Psychopharmacology and Biological Psychiatry*, *92*, 76–82. https://doi.org/10.1016/j.pnpbp.2018.12.017

Han, S., Zheng, R., Li, S., Liu, L., Wang, C., Jiang, Y., Wen, M., Zhou, B., Wei, Y., Pang, J., Li, H., Zhang, Y., Chen, Y., & Cheng, J. (2021). Progressive brain structural abnormality in depression assessed with MR imaging by using causal network analysis. *Psychological Medicine*, *1-10*, 1–10. https://doi.org/10.1017/s0033291721003986

Hearne, L. J., & Lin, H. Y. (2021). ADHD symptoms map onto noise-driven structure–function decoupling between hub and peripheral brain regions. *Molecular Psychiatry*, *26*(8), 4036–4045. https://doi.org/10.1038/s41380-019-0554-6

Honey, C. J., Sporns, O., Cammoun, L., Gigandet, X., Thiran, J. P., Meuli, R., & Hagmann, P. (2009). Predicting human resting-state functional connectivity from structural connectivity. *Proceedings of the National Academy of Sciences of the United States of America*, *106*(6), 2035–2040. https://doi.org/10.1073/pnas.0811168106

Hou, J., Wu, W., Lin, Y., Wang, J., Zhou, D., Guo, J., Gu, S., He, M., Ahmed, S., Hu, J., Qu, W., & Li, H. (2012). Localization of cerebral

functional deficits in patients with obsessive-compulsive disorder: A resting-state fMRI study. *Journal of Affective Disorders*, *138*(3), 313–321. https://doi.org/10.1016/j.jad.2012.01.022

Jiang, H., Zhu, R., Tian, S., Wang, H., Chen, Z., Wang, X., Shao, J., Qin, J., Shi, J., Liu, H., Chen, Y., Yao, Z., & Lu, Q. (2020). Structural-functional decoupling predicts suicide attempts in bipolar disorder patients with a current major depressive episode. *Neuropsychopharmacology*, *45*(10), 1735–1742. https://doi.org/10.1038/s41386-020-0753-5

Kim, J. J., Lee, M. C., Kim, J., Kim, I. Y., Kim, S. I., Han, M. H., Chang, K. H., & Kwon, J. S. (2001). Grey matter abnormalities in obsessive–compulsive disorder: Statistical parametric mapping of segmented magnetic resonance images. *British Journal of Psychiatry the Journal of Mental Science*, *179*(5), 330–334.

Komulainen, K., Airaksinen, J., Savelieva, K., Gluschkoff, K., García Velázquez, R., Elovainio, M., & Jokela, M. (2021). Network dynamics of depressive symptoms in antidepressant medication treatment: secondary analysis of eight clinical trials. *Molecular Psychiatry*, *26*(7), 3328–3335. https://doi.org/10.1038/s41380-020-00884-3

Lázaro, L., Castro-Fornieles, J., Cullell, C., Andrés, S., Falcón, C., Calvo, R., & Bargalló, N. (2011). A voxel-based morphometric MRI study of stabilized obsessive-compulsive adolescent patients. *Progress in Neuro-Psychopharmacology & Biological Psychiatry*, *35*(8), 1863–1869. https://doi.org/10.1016/j.pnpbp.2011.07.016

Lei, D., & Pinaya, W. H. L. (2020). Integrating machining learning and multimodal neuroimaging to detect schizophrenia at the level of the individual. *Human Brain Mapping*, *41*(5), 1119–1135. https://doi.org/10.1002/hbm.24863

Liu, J., Bu, X., Hu, X., Li, H., Cao, L., Gao, Y., Liang, K., Zhang, L., Lu, L., Hu, X., Wang, Y., Gong, Q., & Huang, X. (2021). Temporal variability of regional intrinsic neural activity in drug-naïve patients with obsessive-compulsive disorder. *Human Brain Mapping*, *42*(12), 3792–3803. https://doi.org/10.1002/hbm.25465

Liu, S., Seidlitz, J., Blumenthal, J. D., Clasen, L. S., & Raznahan, A. (2020). Integrative structural, functional, and transcriptomic analyses of sex-biased brain organization in humans. *Proceedings of the National Academy of Sciences of the United States of America*, *117*(31), 18788–18798. https://doi.org/10.1073/pnas.1919091117

Liu, Z., Palaniyappan, L., Wu, X., Zhang, K., du, J., Zhao, Q., Xie, C., Tang, Y., Su, W., Wei, Y., Xue, K., Han, S., Tsai, S. J., Lin, C. P., Cheng, J., Li, C., Wang, J., Sahakian, B. J., Robbins, T. W., … Feng, J. (2021). Resolving heterogeneity in schizophrenia through a novel systems approach to brain structure: individualized structural covariance network analysis. *Molecular Psychiatry*, *26*, 7719–7731. https://doi.org/10.1038/s41380-021-01229-4

Lv, J., di Biase, M., Cash, R. F. H., Cocchi, L., Cropley, V. L., Klauser, P., Tian, Y., Bayer, J., Schmaal, L., Cetin-Karayumak, S., Rathi, Y., Pasternak, O., Bousman, C., Pantelis, C., Calamante, F., & Zalesky, A. (2020). Individual deviations from normative models of brain structure in a large cross-sectional schizophrenia cohort. *Molecular Psychiatry*, *26*, 3512–3523. https://doi.org/10.1038/s41380-020-00882-5

Markello, R. D., Shafiei, G., Tremblay, C., Postuma, R. B., Dagher, A., & Misic, B. (2021). Multimodal phenotypic axes of Parkinson's disease. *NPJ Parkinson's Disease*, *7*(1), 6–12. https://doi.org/10.1038/s41531-020-00144-9

McKay, D., Abramowitz, J. S., Calamari, J. E., Kyrios, M., Radomsky, A., Sookman, D., Taylor, S., & Wilhelm, S. (2004). A critical evaluation of obsessive-compulsive disorder subtypes: Symptoms versus mechanisms. *Clinical Psychology Review*, *24*(3), 283–313. https://doi.org/10.1016/j.cpr.2004.04.003

Menzies, L., Chamberlain, S. R., Laird, A. R., Thelen, S. M., Sahakian, B. J., & Bullmore, E. T. (2008). Integrating evidence from neuroimaging and neuropsychological studies of obsessive-compulsive disorder: The orbitofronto-striatal model revisited. *Neuroscience and Biobehavioral Reviews*, *32*(3), 525–549. https://doi.org/10.1016/j.neubiorev.2007.09.005

Mišić, B., & Sporns, O. (2016). From regions to connections and networks: New bridges between brain and behavior. *Current Opinion in Neurobiology*, *40*, 1–7. https://doi.org/10.1016/j.conb.2016.05.003

Nishida, S., Narumoto, J., Sakai, Y., Matsuoka, T., Nakamae, T., Yamada, K., Nishimura, T., & Fukui, K. (2011). Anterior insular volume is larger in patients with obsessive-compulsive disorder. *Progress in Neuro-Psychopharmacology & Biological Psychiatry*, *35*(4), 997–1001. https://doi.org/10.1016/j.pnpbp.2011.01.022

Okada, K., Nakao, T., Sanematsu, H., Murayama, K., Honda, S., Tomita, M., Togao, O., Yoshiura, T., & Kanba, S. (2015). Biological heterogeneity of obsessive-compulsive disorder: A voxel-based morphometric study based on dimensional assessment. *Psychiatry and Clinical Neurosciences*, *69*(7), 411–421. https://doi.org/10.1111/pcn.12269

Okasha, A., Rafaat, M., Mahallawy, N., El Nahas, G., El Dawla, A. S., Sayed, M., & El Kholi, S. (2000). Cognitive dysfunction in obsessive-compulsive disorder. *Acta Psychiatrica Scandinavica*, *101*(4), 281–285.

Ota, M., Ishikawa, M., Sato, N., Hori, H., Sasayama, D., Hattori, K., Teraishi, T., Noda, T., Obu, S., Nakata, Y., Higuchi, T., & Kunugi, H. (2013). Discrimination between schizophrenia and major depressive disorder by magnetic resonance imaging of the female brain. *Journal of Psychiatric Research*, *47*(10), 1383–1388. https://doi.org/10.1016/j.jpsychires.2013.06.010

Pujol, J., Soriano-Mas, C., Alonso, P., Cardoner, N., Menchón, J. M., Deus, J., & Vallejo, J. (2004). Mapping structural brain alterations in obsessive-compulsive disorder. *Archives of General Psychiatry*, *61*(7), 720–730. https://doi.org/10.1001/archpsyc.61.7.720

Rai, N., Negi, S., Chaudhury, S., & Deshmukh, O. (2017). Partial multi-view clustering using graph regularized NMF. In *Paper presented at the 2016 23rd International Conference on Pattern Recognition (ICPR)*. IEEE. https://doi.org/10.1109/ICPR.2016.7899961

Ravindran, A., Richter, M., Jain, T., Ravindran, L., Rector, N., & Farb, N. (2020). Functional connectivity in obsessive-compulsive disorder and its subtypes. *Psychological Medicine*, *50*(7), 1173–1181. https://doi.org/10.1017/s0033291719001090

Rotge, J. Y., Guehl, D., Dilharreguy, B., Tignol, J., Bioulac, B., Allard, M., Burbaud, P., & Aouizerate, B. (2009). Meta-analysis of brain volume changes in obsessive-compulsive disorder. *Biological Psychiatry*, *65*(1), 75–83. https://doi.org/10.1016/j.biopsych.2008.06.019

Saxena, S., Brody, A. L., Schwartz, J. M., & Baxter, L. R. (1998). Neuroimaging and frontal-subcortical circuitry in obsessive-compulsive disorder. *The British Journal of Psychiatry*, *35*, 26–37.

Saxena, S., & Rauch, S. L. (2000). Functional neuroimaging and the neuroanatomy of obsessive-compulsive disorder. *The Psychiatric Clinics of North America*, *23*(3), 563–586. https://doi.org/10.1016/s0193-953x(05)70181-7

Shen, X., Tokoglu, F., Papademetris, X., & Constable, R. T. (2013). Groupwise whole-brain parcellation from resting-state fMRI data for network node identification. *NeuroImage*, *82*, 403–415. https://doi.org/10.1016/j.neuroimage.2013.05.081

Skudlarski, P., Jagannathan, K., Anderson, K., Stevens, M. C., Calhoun, V. D., Skudlarska, B. A., & Pearlson, G. (2010). Brain connectivity is not only lower but different in schizophrenia: A combined anatomical and functional approach. *Biological Psychiatry*, *68*(1), 61–69. https://doi.org/10.1016/j.biopsych.2010.03.035

Soriano-Mas, C. (2021). Functional brain imaging and OCD. *Current Topics in Behavioral Neurosciences*, *49*, 269–300. https://doi.org/10.1007/7854_2020_203

Starcevic, V., & Brakoulias, V. (2008). Symptom subtypes of obsessive-compulsive disorder: Are they relevant for treatment? *The Australian and New Zealand Journal of Psychiatry*, *42*(8), 651–661. https://doi.org/10.1080/00048670802203442

Stein, D. J., Costa, D. L. C., Lochner, C., Miguel, E. C., Reddy, Y. C. J., Shavitt, R. G., van den Heuvel, O. A., & Simpson, H. B. (2019). Obsessive-compulsive disorder. *Nature Reviews Disease Primers*, *5*(1), 52. https://doi.org/10.1038/s41572-019-0102-3

Strehl, A., & Ghosh, J. (2003). Cluster ensembles -- a knowledge reuse framework for combining multiple partitions. *Journal of Machine Learning Research*, *3*, 583–617.

Subirà, M., Alonso, P., Segalàs, C., Real, E., López-Solà, C., Pujol, J., Martínez-Zalacaín, I., Harrison, B. J., Menchón, J. M., Cardoner, N., & Soriano-Mas, C. (2013). Brain structural alterations in obsessive-compulsive disorder patients with autogenous and reactive obsessions. *PLoS One*, *8*(9), e75273. https://doi.org/10.1371/journal.pone.0075273

Sui, J., Qi, S., van Erp, T. G. M., Bustillo, J., Jiang, R., Lin, D., Turner, J. A., Damaraju, E., Mayer, A. R., Cui, Y., Fu, Z., du, Y., Chen, J., Potkin, S. G., Preda, A., Mathalon, D. H., Ford, J. M., Voyvodic, J., Mueller, B. A., … Calhoun, V. D. (2018). Multimodal neuromarkers in schizophrenia via cognition-guided MRI fusion. *Nature Communications*, *9*(1), 3028. https://doi.org/10.1038/s41467-018-05432-w

Sun, X., Liu, J., Ma, Q., Duan, J., Wang, X., Xu, Y., Xu, Z., Xu, K., Wang, F., Tang, Y., He, Y., & Xia, M. (2021). Disrupted Intersubject variability architecture in functional connectomes in schizophrenia. *Schizophrenia Bulletin*, *47*(3), 837–848. https://doi.org/10.1093/schbul/sbaa155

Sundermann, B., Olde Lütke Beverborg, M., & Pfleiderer, B. (2014). Toward literature-based feature selection for diagnostic classification: A meta-analysis of resting-state fMRI in depression. *Frontiers in Human Neuroscience*, *8*, 692. https://doi.org/10.3389/fnhum.2014.00692

Swedo, S. E., Pietrini, P., Leonard, H. L., Schapiro, M. B., Rettew, D. C., Goldberger, E. L., Rapoport, S. I., Rapoport, J. L., & Grady, C. L. (1992). Cerebral glucose metabolism in childhood-onset obsessive-compulsive disorder. Revisualization during pharmacotherapy. *Archives of General Psychiatry*, *49*(9), 690–694. https://doi.org/10.1001/archpsyc.1992.01820090018003

Szeszko, P. R., Christian, C., MacMaster, F., Ph.D., Lencz, T., Mirza, Y., Taormina, S. P., Easter, P., B.A., Rose, M., B.A., Michalopoulou, G. A., Ph.D., & Rosenberg, D. R., M.D. (2008). Gray matter structural alterations in psychotropic drug-naive pediatric obsessive-compulsive disorder: An optimized voxel-based morphometry study. *The American Journal of Psychiatry*, *165*(10), 1299–1307. https://doi.org/10.1176/appi.ajp.2008.08010033

van den Heuvel, O. A., Remijnse, P. L., Mataix-Cols, D., Vrenken, H., Groenewegen, H. J., Uylings, H. B., van Balkom, A. J. L. M., & Veltman, D. J. (2009). The major symptom dimensions of obsessive-compulsive disorder are mediated by partially distinct neural systems. *Brain*, *132*(Pt 4), 853–868. https://doi.org/10.1093/brain/awn267

Varol, E., Sotiras, A., & Davatzikos, C. (2017). HYDRA: Revealing heterogeneity of imaging and genetic patterns through a multiple max-margin discriminative analysis framework. *NeuroImage*, *145*, 346–364. https://doi.org/10.1016/j.neuroimage.2016.02.041

Veltman, D. J. (2021). Structural imaging in OCD. *Current Topics in Behavioral Neurosciences*, *49*, 201–229. https://doi.org/10.1007/7854_2020_209

Voineskos, A. N., Jacobs, G. R., & Ameis, S. H. (2020). Neuroimaging heterogeneity in psychosis: Neurobiological underpinnings and opportunities for prognostic and therapeutic innovation. *Biological Psychiatry*, *88*(1), 95–102. https://doi.org/10.1016/j.biopsych.2019.09.004

Wang, B., Mezlini, A. M., Demir, F., Fiume, M., Tu, Z., Brudno, M., & Haibe-Kains, B. (2014). Similarity network fusion for aggregating data types on a genomic scale. *Nature Methods*, *11*(3), 333–337. https://doi.org/10.1038/nmeth.2810

Wolfers, T., Beckmann, C. F., Hoogman, M., Buitelaar, J. K., Franke, B., & Marquand, A. F. (2020). Individual differences v.the average patient: Mapping the heterogeneity in ADHD using normative models. *Psychological Medicine*, *50*(2), 314–323. https://doi.org/10.1017/s0033291719000084

Wolfers, T., Doan, N. T., Kaufmann, T., Alnæs, D., Moberget, T., Agartz, I., Buitelaar, J. K., Ueland, T., Melle, I., Franke, B., Andreassen, O. A., Beckmann, C. F., Westlye, L. T., & Marquand, A. F. (2018). Mapping the heterogeneous phenotype of schizophrenia and bipolar disorder using normative models. *JAMA Psychiatry*, *75*(11), 1146–1155. https://doi.org/10.1001/jamapsychiatry.2018.2467

Xia, J., Fan, J., Liu, W., Du, H., Zhu, J., Yi, J., Tan, C., & Zhu, X. (2020). Functional connectivity within the salience network differentiates autogenous- from reactive-type obsessive-compulsive disorder. *Progress in Neuro-Psychopharmacology & Biological Psychiatry*, *98*, 109813. https://doi.org/10.1016/j.pnpbp.2019.109813

Yoo, S. Y., Roh, M. S., Choi, J. S., Kang, D. H., Ha, T. H., Lee, J. M., Kim, I. Y., Kim, S. I., & Kwon, J. S. (2008). Voxel-based morphometry study of gray matter abnormalities in obsessive-compulsive disorder. *Journal of Korean Medical Science*, *23*(1), 24–30. https://doi.org/10.3346/jkms.2008.23.1.24

Yu-Feng, Z., Yong, H., Chao-Zhe, Z., Qing-Jiu, C., Man-Qiu, S., Meng, L., Li-Xia, T., Tian-Zi, J., & Yu-Feng, W. (2007). Altered baseline brain activity in children with ADHD revealed by resting-state functional MRI. *Brain and Development*, *29*(2), 83–91. https://doi.org/10.1016/j.braindev.2006.07.002

SUPPORTING INFORMATION

Additional supporting information can be found online in the Supporting Information section at the end of this article.

How to cite this article: Han, S., Xu, Y., Guo, H.-R., Fang, K., Wei, Y., Liu, L., Cheng, J., Zhang, Y., & Cheng, J. (2022). Two distinct subtypes of obsessive compulsive disorder revealed by a framework integrating multimodal neuroimaging information. *Human Brain Mapping*, *43*(14), 4254–4265. https://doi.org/10.1002/hbm.25951